DYNAMICS OF A REAL TRIPLE PENDULUM - MODELING AND EXPERIMENTAL OBSERVATION

Jan Awrejcewicz and Grzegorz Kudra
Department of Automatics and Biomechanics
Technical University of Łódź
Poland
awrejcew@p.lodz.pl

Abstract

Nonlinear dynamics of a real plane and periodically forced triple pendulum is investigated both experimentally and numerically. Mathematical modeling includes details taking into account some characteristic features as well as some imperfections of the real system. Parameters of the model are obtained by estimation from the experimental data. Then the experimental and numerical analysis of the system is performed.

Key words

triple pendulum, identification, chaos, dry friction modeling, mathematical modeling

1 Introduction

A pendulum as a simple nonlinear systems is still a subject of interest of scientists from all the world. It is caused by simplicity of that system on the one hand, and due to many fundamental and spectacular phenomena exhibited by a single pendulum on the other hand. In mechanics and physics investigations of single and coupled pendulums are widely applied. Lately, even the monograph on the pendulum has been published [Baker, 2005]. This is a large study on this simple system also from the historical point of view.

Although a single or a double pendulum (in their different forms) are quite often studied experimentally [Blackburn et al., 1987; Bishop and Sudor, 1998], a triple physical pendulum is rather rarely presented in literature from a point of view of real experimental object. For example, in the work [Zhu and Ishitobi, 1999] the triple pendulum excited by horizontal harmonic motion of the pendulum frame is presented and a few examples of chaotic attractors are reported. Experimental rigs of any pendulums are still of interest of many researchers dealing with dynamics of continuous multi degrees-of-freedom mechanical systems. The model having such a properties has been analyzed in work [Galan et al., 2005] It consists of a chain of N identical pendulums coupled by dumped elastic joints subject to vertical sinusoidal forcing on its base.

In February, 2005, in the Department of Automatics and Biomechanics, the experimental rig of triple physical pendulum was finished and activated. This stand has been constructed and built in order to investigate experimentally various phenomena of nonlinear dynamics, including regular and chaotic motions, bifurcations, coexisting attractors, etc. In order to have more deep insight into dynamics of the real pendulum, the corresponding mathematical model is required. In the work [Awrejcewicz et al., 2005] the suitable mathematical modeling and numerical analysis have been performed, where the viscous damping in the pendulum joints (constructed by the use of rolling bearings) has been assumed. In the next step [Awrejcewicz et al., 2008], we have also taken into account the dry friction in the joints with many details and variants. Here we present the model of friction taking into account only essential details.

2 Experimental rig

The experimental rig (see Fig. 1) of the triple physical pendulum consists of the following subsystems: pendulum, driving subsystem and the measurement subsystem. It is assumed that the pendulum is moving in a plane.

The links (1, 2, 3) are suspended on the frame (4) and joined by the use of radial and axial needle bearings. The first link is forced by a special direct-current motor of our own construction with optical commutation consisting of two stators (6) and two rotors (5). The construction ensures avoiding the skewing of the structure and forming the forces and moments in planes different that the plane of the assumed pendulum motion. On the other hand the construction allows the full rotations of all the links of the pendulum.

The voltage conveyed to the engine inductors is controlled by the use of special digital system of our own construction together with precise signal genera-

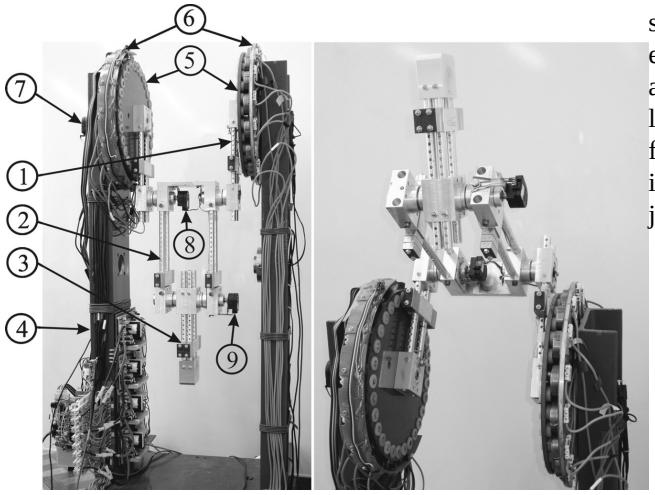

Figure 1. Experimental rig: 1, 2, 3 - links; 4 - stand; 5 - rotors; 6 - stators; 7, 8, 9 - rotational potentiometers.

tor HAMEG. As a result the square-shape in time forcing (but with some assymmetry - see the next sections) with adjustable frequency and desired amplitude is obtained.

The measurement of the angular position of the three links is realized by the use of the precise rotational potentiometers (7, 8, 9). Then the LabView measure-programming system is used for experimental data acquisition and presentation on a computer.

3 Mathematical model

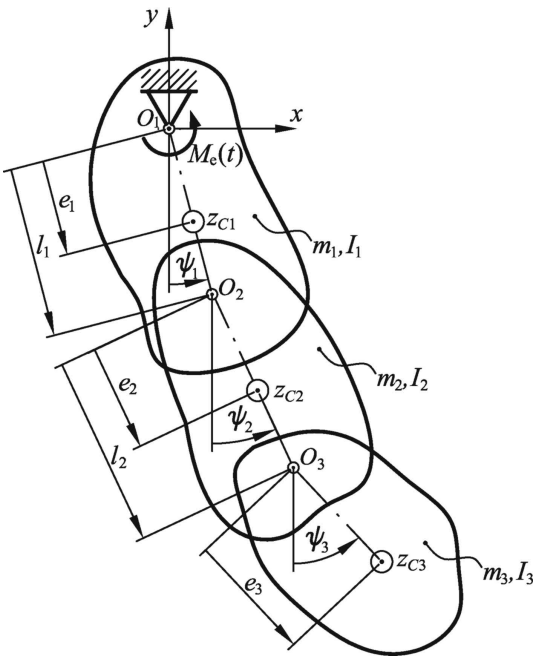

Figure 2. Physical model.

Details on physical modeling, i.e. idealized physical concept (presented in Fig. 2) of real pendulum presented in Fig. 1, can be found in works [Awrejcewicz et al., 2005; **?**]. The system is idealized since it is assumed that it is an ideally plane system of coupled links, moving in the vacuum with the assumed model of friction in joints. The system is governed by the following set of differential equations (for more see [Awrejcewicz et al., 2005; **?**]):

$$\begin{bmatrix} B_1 & N_{12}c_{12} & N_{13}c_{13} \\ N_{12}c_{12} & B_2 & N_{23}c_{23} \\ N_{13}c_{13} & N_{23}c_{23} & B_3 \end{bmatrix} \begin{Bmatrix} \ddot{\psi}_1 \\ \ddot{\psi}_2 \\ \ddot{\psi}_3 \end{Bmatrix} +$$

$$+ \begin{bmatrix} 0 & N_{12}s_{12} & N_{13}s_{13} \\ -N_{12}s_{12} & 0 & N_{23}s_{23} \\ -N_{13}s_{13} & -N_{23}s_{23} & 0 \end{bmatrix} \begin{Bmatrix} \dot{\psi}_1^2 \\ \dot{\psi}_2^2 \\ \dot{\psi}_3^2 \end{Bmatrix} +$$

$$+ \begin{Bmatrix} M_{R1} - M_{R2} \\ M_{R2} - M_{R3} \\ M_{R3} \end{Bmatrix} + \begin{Bmatrix} M_1 \sin\psi_1 \\ M_2 \sin\psi_2 \\ M_2 \frac{N_{13}}{N_{12}} \sin\psi_3 \end{Bmatrix} = \begin{Bmatrix} M_e(t) \\ 0 \\ 0 \end{Bmatrix}. \quad (1)$$

where the pendulum position is described by the use of three angles ψ_i ($i = 1, 2, 3$) and where

$$c_{ij} = \cos(\psi_i - \psi_j), s_{ij} = \sin(\psi_i - \psi_j), \quad (2)$$

and

$$M_{R1} = T_1 \frac{2}{\pi} \arctan(\varepsilon\dot{\psi}_1) + 2c\dot{\psi}_1,$$
$$M_{R2} = T_2 \frac{2}{\pi} \arctan\Big(\varepsilon(\dot{\psi}_2 - \dot{\psi}_1)\Big) + c(\dot{\psi}_2 - \dot{\psi}_1),$$
$$M_{R3} = T_3 \frac{2}{\pi} \arctan\Big(\varepsilon(\dot{\psi}_3 - \dot{\psi}_2)\Big) + c(\dot{\psi}_3 - \dot{\psi}_2), \quad (3)$$

are the moments of resistance in the corresponding joints and consinsting of two parts: dry friction and viscous damping. The dry friction moment does not depend on the loading of the corresponding bearing and the sign function is approximated by the arctan function. The parameter c is the damping coefficient common for the second and third joint while in the first joint we assume damping two times greater (since the first joint is built by the use of four bearings, while each other joint contain two bearings).

In the work [Awrejcewicz et al., 2008] more complex model of friction has been investigated where the dry friction moment consists of two part: the first one proportional to the normal loading in the bearing and the second one beeing constant (and present also in the lack of loading). Moreover the friction is a function of relative velocity due to the Stribeck's curve. As a result of those investigations we have concluded that in our case the model of friction can be simplified to the one presented by the Eq. (3), without any loss of precision.

The external excitation in the pendulum model can be an arbitrary time function, and in particular, it can be the same function as applied (and recorded to a file) in real system (it is useful in the parameter estimation

process). On the other hand, it is possible to apply a forcing due to the following mathematical description:

$$M_e(t) = \begin{cases} q & \text{if } \omega t + \phi_0 \mod 2\pi \leq 2\pi a \\ -q & \text{if } \omega t + \phi_0 \mod 2\pi > 2\pi a \end{cases}, \quad (4)$$

which imitates the square-shape in time forcing (applied in the real pendulum), with adjustable angular velocity ω, initial phase ϕ_0, amplitude q and the coefficient a (for $a \neq 0.5$ there is an asymmetry in the forcing, as mentioned in section 2).

4 Model parameters

Table 1. Parameter estimations.

	A_1	B_1	C_1
B_1 [kg·cm^2]	1650.3	1634.7	1641.3
B_2 [kg·cm^2]	1386.3	1378.7	1390.9
B_3 [kg·cm^2]	163.32	166.56	164.50
N_{12} [kg·cm^2]	1111.2	1104.5	1112.6
N_{12} [kg·cm^2]	198.99	201.47	199.92
N_{23} [kg·cm^2]	255.96	259.16	257.15
M_1 [N·cm]	879.76	874.38	875.00
M_2 [N·cm]	632.37	628.53	633.13
T_1 [N·mm]	56.83	72.73	97.53
T_2 [N·mm]	25.06	15.16	13.77
T_3 [N·mm]	11.07	4.58	6.61
c [N·mm·s]	*0*	1.057	0.532
ε [s]	*1000*	*1000*	6.77
$10^3 \cdot F_{cr}$ [rad^2]	0.3255	0.3059	0.2809

The model parameters are estimated by the global minimum searching of the criterion-function of the model and real system matching. The matching of model and real system is understood as the matching of the corresponding output signals $\psi_i(t)$ (i =1,2,3) from model integrated numerically and from the real pendulum, assuming the same inputs to both model and real system. The sum of squares of deviations between corresponding samples of signals from model and experiment, for few different solutions, serves as a criterion function. Together with the model parameters also initial conditions of the numerical simulation are estimated. A minimum is searched applying the simplex method. In order to avoid the local minima, the simplex method is stopped from time to time and a random searching is then applied. After random searching the simplex method is restarted again.

If we divide final value of criterion-function by the number of samples used in calculation of criterion-function, we obtain average square of deviation between two signals (obtained from the model and the experiment) - let us denote this parameter as F_{cr}. Now this parameter can be used for comparison of matching of different sets of experimental data and corresponding numerical solutions.

In the Table 1 the part of the results of the parameter estimations performed in the work [Awrejcewicz et al., 2008] is presented. Three different sets of parameters are presented, correspondingly to three variants of the model of resistance in the joints. The set A_1 corresponds to the model with dry friction only. The model B_1 contains also viscous damping. The next model (C_1) is a development of the previous one (B_1): the parameter ε is added to the set of the identified parameters.

In all the identification processes, the same set of experimental solutions is used: five periodic solutions with the forcing frequencies ($f = \omega/2\pi$): $f = 0.2$, 0.35, 0.6, 0.85 and 1.1 Hz (for each the solution the 20 sec of motion was recorded, after ignoring the transient motions) and one decaying solution, which starts from the periodic attractor with forcing frequency $f = 0.5$ Hz (after few seconds of the recorded motion, the forcing was switched off and the total length of the recorded motion was 24 sec). Note that in our work, we do not measure actual value of the forcing, but only the control signal is recorded (determining the sign of the forcing), since we assume the constant forcing amplitude $q = 1.718$ Nm (determined before the identification experiments).

5 Simulation results

In the upper part of Fig. 3 the final model C_1 and real system matching for vanishing motion (started from the periodic attractor with the forcing frequency $f = 0.5$ Hz), obtained during the identification process, is presented. In this scale we see almost perfect matching of the corresponding behaviors. The bottom part of Fig. 3 presents enlargement of the final phase of decaying of the same motion, where in addition the simulation of the model A_1 is shown. Here we can observe in details certain aspect of the difference between models A_1 and C_1.

Figure 4 show results of investigation of the forcing frequency region 0.13-0.14 Hz. It is an example that the developed model with their parameters can predict real pendulum dynamics exhibited also for forcing frequencies f outside the region 0.2-1.1 Hz (containing all the periodic solutions taken to the identification process).

6 Conclusion

Few versions of the model of resistance in the joints have been tested in the identification process. Good agreement between both numerical simulation results and experimental measurements have been obtained

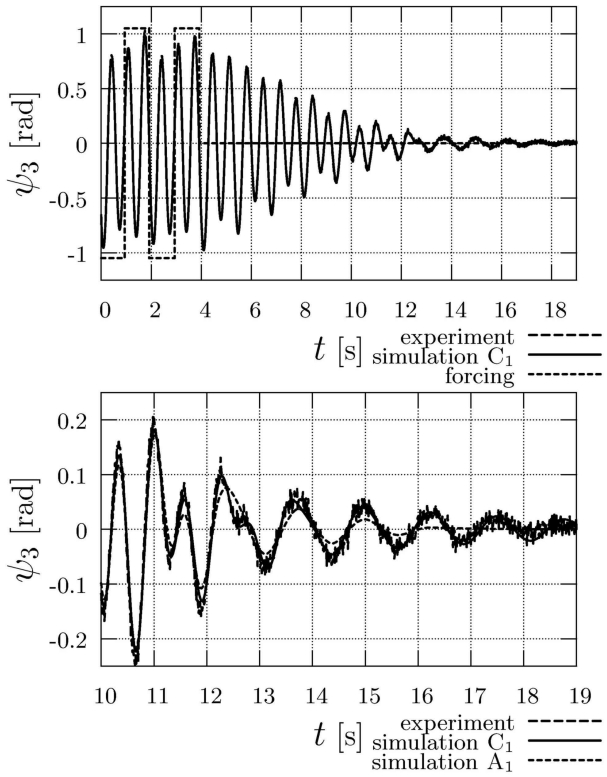

Figure 3. Final model (C_1 and A_1) and real system matching for vanishing motion

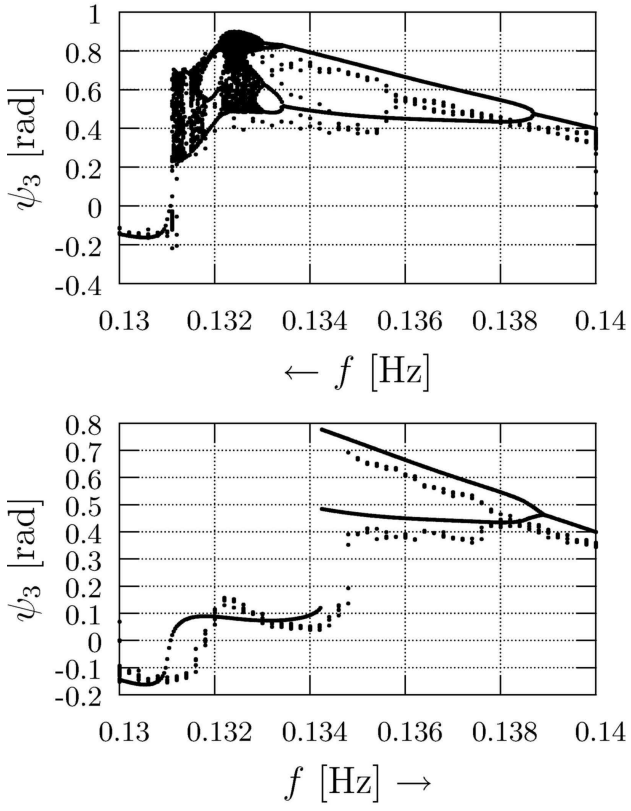

Figure 4. Bifurcation diagrams exhibited by experiment and model (C_1) with the parameter f growing ($\rightarrow$) and decreasing ($\leftarrow$).

and presented, for all the variants of the friction model. However, one of them, namely C_1, seems to be optimal, since it gives relatively good results with simultaneous simplicity of the model itself, and high speed of the simulation.

The model C_1 is better for simulation (higher simulation speed) than others because the ε parameter is much smaller and the characteristic of the friction torque are is smooth. It is interesting that model C_1 give better results than models B_1, while the only modification is the parameter ε treated as identified one (the result is the smaller value of the parameter ε). We are not able to give a physical interpretation of that at this moment. But since it is important to have a model giving results close to experimental observations, we can accept even some artificial improvements of the model having only functional role, no physical sense, particularly if they speed up the simulation process.

I should be noted, that examples of numerical and experimental simulations presented is section 5 are selective. However, the presented examples show quite good agreement between numerical and experimental results. It leads to conclusion that the used mathematical model of triple pendulum with its parameters estimated can be applied as a tool for quick searching for various phenomena of nonlinear dynamics exhibited by a real pendulum as well as for explanation of its rich dynamics.

Acknowledgements

This work has been supported by the Ministry of Science and Information (grant No 4 T07A 031 28).

References

Baker, G. L. and Blackburn, J. A. (2005). *The Pendulum. A Case Study in Physics*. Oxford University Press.

Blackburn, J. A., Zhou-Jing, Y., Vik, S., Smith, H .J. T. and Nerenberg, M.A.H. (1987). Experimental study of chaos in a driven pendulum. *Physica* **D26**(1-3), pp. 385-395.

Bishop, S. R. and Sudor, D. J. (1998). The "not quite" inverted pendulum. *International Journal of Bifurcation and Chaos* **9**(1), pp. 273-285.

Zhu, Q. and Ishitobi, M. (1999). Experimental study of chaos in a driven triple pendulum. *Journal of Sound and Vibration* **227**(1), pp. 230-238.

Galan, J., Fraser, W. B., Acheson, D. J. and Champneys A. R. (2005). The parametrically excited upside-down rod: an elastic jointed pendulum model. *Journal of Sound and Vibration* 280, pp. 359-377.

Awrejcewicz, J., Kudra, G. and Wasilewski, G. (2005). Experimental and numerical investigation of chaotic zones exhibited by the triple physical pendulum. In *Proceedings of the 8th Conference on Dynamical Systems - Theory and Applications* Łódź, pp. 183-188.

Awrejcewicz, J., Supeł, B., Kudra, G., Wasilewski, G. and Olejnik, P.(2008). Numerical and experimental

study of regular and chaotic motion of triple physical pendulum. *International Journal of Bifurcation and Chaos* **18**(10), to appear.